



# An optoelectronic detector for elastic and diffractive scattering measurements in the TOTEM experiment at the LHC

M. Buénerd\*, J. Pouxé, C. Vescovi

*Institut des Sciences Nucléaires, IN2P3/CNRS, 53, Avenue des Martyrs, 38026 Grenoble-cedex, France*

## Abstract

An optoelectronic detector based on a fast phosphor scintillator optically coupled to an image intensifier combined with a CMOS photosensitive array is described and discussed in the perspective of elastic and diffractive scattering measurement in the TOTEM experimental program at the CERN LHC. © 2000 Elsevier Science B.V. All rights reserved.

## 1. Introduction

The elastic and diffractive scattering studies in the TOTEM experiment at the LHC will consist of detecting scattered particles transported by the dedicated parallel-to-point-focussing (PPF) optics [1], and performing accurate position measurements of these particles. These measurements will have to be achieved down to very close (transverse) distance from the collider beam, in order to get as close as possible to the Coulomb–Nuclear interference region of the proton–proton scattering amplitude. An estimate of the value of this critical distance is about 2 mm, corresponding to a  $15\sigma + 0.5$  mm distance from the beam axis ( $\sigma$ , standard deviation of transverse beam distribution in the detector plane along the axis of measurement) [2].

Because of this particular experimental situation, the detection system to be implemented has to

comply with a set of drastic requirements. In particular, the detectors should:

- (1) Have a spatial resolution of the order of 30  $\mu\text{m}$  in the transverse direction from the beam, along the axis of measurement, over an area of at least  $2 \times 2 \text{ cm}^2$ .
- (2) Have a minimal dead zone on their near beam edge, in order to minimize the radial range not accessible to measurement because of the presence of matter.
- (3) Have a low sensitivity to the electromagnetic background generated by very nearby beam bursts.
- (4) Be radiation hard, inexpensive and conveniently interchangeable. This latter condition originating from the proximity to the beam which instabilities, even small, could be very damaging or even fatal for most usual detectors.
- (5) Have a counting rate capability which can be estimated in the range of at least  $10^4 \text{ s}^{-1}$  for the expected experimental conditions, for physical plus background events, on the basis of UA4 experience [3–5].

\*Corresponding author.

E-mail address: buenerd@in2p3.fr (M. Buénerd)

Most usual detectors, such as silicon microstrips or gas counters (MWPC, MSGC), etc., fail to satisfy one or more of these conditions.

This contribution outlines a scenario of detector which would excellently meet all the above requirements. The next section describes the conceptual design of the device. The following sections investigate the properties of the individual components considered for the apparatus, and their ability to provide the expected performances. Section 3 deals with the fast phosphor material required for the primary scintillator function, whereas the simple optical focusing device needed in the apparatus is discussed in Section 4, the Image Intensifier (II) in Section 5, and the CMOS photodetector in Section 6. The mechanical aspects are outlined in Section 8 before the conclusion is given.

## 2. Conceptual design

Fig. 1 shows schematically the design principle of the detector. The primary detection stage is made of a simple layer of fast phosphor (PH) deposited on a plaquette of solid material (metal or ceramics). The phosphor layer could be covered or not with an optical fiber window to collimate the photons. A fraction of the photons radiated by the phosphor is collected and transported by a simple optical system and focused on the photocathode of an II, with a variable magnification. The latter gives a convenient flexibility to the apparatus. The II is optically coupled to a CMOS photodetector array which provides the position measurement. This device is in a way, nothing else than a dedicated intensified CMOS camera whose elements are arranged in a geometry matching the experimental constraints.

It is easy to see that such a detection system would meet all the requirements listed previously. Indeed, the primary radiator would have no dead zone on the near-beam side and would be active from its extreme edge (some loss of light should be expected however for events hitting the very edge of the radiator, see below). In addition, since it would consist of a simple thin layer of phosphor, it would be inexpensive and interchangeable at minimal cost in case of damage undergone by direct encounter

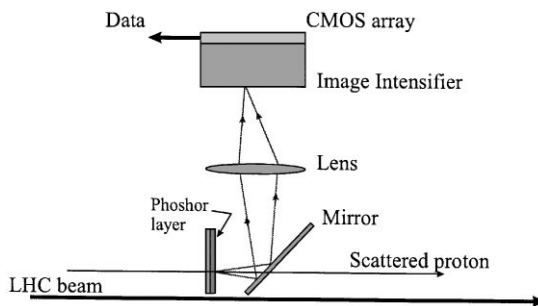


Fig. 1. Schematic view of the design principle.

with the beam in case of possible accidents of the optical stability of the collider. It would also be highly insensitive to the electromagnetic background generated by beam bursts passing nearby. Finally, an overall spatial resolution of the order of 30  $\mu\text{m}$  could easily be obtained for the whole detector since each element could provide an individual performance significantly better than the required value, as seen below. In the following sections, each component of the detector is discussed in terms of its expected performances, availability, and feasibility.

## 3. Phosphor scintillator

The primary scintillator is a key element of the device. It has to meet the three conditions of spatial resolution, primary photon generation with an intensity allowing a high detection efficiency, and decay time of light emission compatible with the required counting rate and timing accuracy. These points are discussed below.

### 3.1. Spatial resolution

The spatial resolution of the scintillator is the size of the bright spot created by the crossing of a particle through the phosphor layer. This issue is well documented in the literature (see Fig. 10.9 in Ref. [6]). A rule of the thumb is that the spot size is roughly equal to the twice the thickness of the phosphor layer.

It will be seen below that a 10  $\mu\text{m}$  thick layer would provide a comfortable number of photons.

The spot size should therefore be about two-thirds of the required spatial accuracy of 30  $\mu\text{m}$ , the corresponding resolution being better than the quoted number in account of the expected Gaussian distribution of the light inside the spot, which could be resolved with fine enough pixels. A significantly better precision than required could then be obtained from this element.

### 3.2. Timing properties

The class of materials considered here is widely used in display screen technology and therefore widely available commercially [6,7]. In order to match the fast timing requirement set by the expected high level of background particles, the scintillator has to be fast decaying, say, on the 10–100 ns scale. Only a few materials are satisfying this condition. Among those are the P46 ( $\text{Y}_3\text{Al}_5\text{O}_{12}:\text{Ce}$ ) and P47 ( $\text{Y}_2\text{SiO}_5:\text{Ce}$ ) commonly used phosphor scintillators (see Refs. [6,7] for other materials not quoted here).

### 3.3. Photon yield, angular and spectral distribution

The photon yield of phosphors is usually quite high compared to usual organic scintillators, at least by an order of magnitude. The yield however varies quite substantially from one phosphor material to another (see Fig. 10.1 in Ref. [6]), slow phosphors providing usually larger yields at longer wavelengths. For the present needs however, it seems that even a fast decaying phosphor would provide enough photons for a high detection efficiency to be obtained.

The P46 and P47 spectral features are summarized in Table 1. The P47 is probably more suitable for the TOTEM detector than the P46, since its decay time is about twice shorter and its light emission peaks in the region of maximum

sensitivity of bialkali photocathodes. The P47 phosphor has been successfully operated in an II used by the authors in a high-resolution beam Cherenkov counter [8]. The light yield of the P46 is larger however. The issue has to be studied exhaustively before the appropriate choice can be made. For a given phosphor, the number of emitted photons can be calculated by integrating the spectral yield distribution  $S(\lambda)$ , usually given in  $\text{W}/(\text{W nm})$ , i.e., Watts of radiated photon energy per nm of wavelength per Watt of energy deposit in the medium. This can be written as

$$N = \int_0^\infty \frac{S(\lambda)}{2\pi\hbar c/\lambda} d\lambda, \quad (1)$$

with  $2\pi\hbar c = 1.24$  (keV nm). For the P47, one gets about 22 radiated photons per keV of energy deposit in the phosphor layer. For a 10  $\mu\text{m}$  thick layer of scintillator, assuming the layer to be homogeneous, and a specific energy loss of about 2 keV/mg/cm<sup>2</sup>, the light yield for 7 TeV protons would be of the order of 440 photons. The angular acceptance and the transmission factor of the optical system, and the quantal efficiency of the II photocathode, would result in a number of photoelectrons as a small fraction of this primary photon yield. It is expected however that this number of produced photoelectrons would be large enough to ensure a safe event signature.

The angular distribution of the photons follows a Lambertian-type law, i.e., varies as  $\cos\theta$  with respect to the particle direction [9]. This forward peaking of the light distribution is particularly convenient for the application considered here.

## 4. Optics

The optical system would consist of a simple spherical lens as illustrated in Fig. 1. A more

Table 1

Characteristics of some fast phosphor candidates. Decay times correspond to the time of decrease of brightness to 10% of its maximum

Reference	Material	Decay time (ns)	Emission peak (nm)	Comments
P46	$\text{Y}_3\text{Al}_5\text{O}_{12}:\text{Ce}$	160	$\approx 550$	Green–yellow
P47	$\text{Y}_2\text{SiO}_5:\text{Ce}$	80	420	Blue–violet

sophisticated system incorporating corrections for geometric aberrations, could be considered in case a large solid angle should be covered for a larger light collection (large lens aperture). No chromatic correction should be needed for the lens since the phosphors considered have almost monochromatic spectral emission.

The flat mirror at  $45^\circ$  does not suffer any particular requirements. It should be of standard laboratory quality for planicity and rugosity.

## 5. Image intensifier

The II would fulfill the two functions of light intensification and of wavelength shifting. Indeed, fast phosphors radiate in the blue, i.e., at wavelengths significantly away from the maximum of the silicon-type photodetector spectral sensitivity which rides over the red-infrared region. A serious mismatch in wavelength would then occur from using a fast phosphor scintillator directly coupled to a silicon photodetector. This mismatch can be conveniently turned around by means of an II which can be equipped with a photocathode (PK) having a range of sensitivity matching that of the primary phosphor spectrum. The output phosphor of the II could then be better matched to the sensitivity of the CMOS array. Practically, with a P47 primary phosphor emitting close to 420 nm, the II should have a multialkali PK which has a maximum sensitivity in this region. The output phosphor of the II could be chosen among longer wavelength emitters and be better matched to the Si sensitivity. Unfortunately, the longer the phosphor wavelength, the longer the characteristic decay time, and phosphors emitting in the red are unacceptably slow for our purpose. A compromise must then be made. P36 for example, would be a reasonable choice compatible both with the spectral and short decay time requirement. The size requirement ( $> 2 \times 2 \text{ cm}^2$ ) can be easily satisfied with commercially available products.

The low level of sensitivity of silicon photosensors (few  $10^2$  photons for CCD-type arrays, practically several  $10^4$  for CMOS-type devices [10]), requires the II to incorporate an intermediate am-

plification stage. This can be achieved by means of one or several micro-channel plates (MCP) in second generation IIs, and allows to reach easily the appropriate light gain ( $10^4$  photons per incident photoelectron), at the price of some loss of spatial resolution however.

In addition, the II technique offers the flexibility of being gatable at a time scale of the order of 50 ns. This allows the event processing to be protected against pile-up events by means of a fast trigger controlled gating voltage.

## 6. CMOS array and readout electronics

The CCD technique offers a convenient and proven way of recording the phosphor image and of reading out the device. However, the technique suffers some significant handicap. All channels are necessarily readout in the sequence, and the readout time is normally very long, at the scale of 10–20 ms (for  $10^3 \times 10^3$  channels). However, it could be made marginally compatible with the present count rate requirements by using a line-by-line type of parallel readout architecture.

### 6.1. CMOS array

The very simple topology of the elastic events (one hit or hit cluster above a given threshold per event) allows fast readout architectures to be considered if individual pixels could be read independently. In this context, the newly developed CMOS technique [10] offers a potentially much better suitability to the needs of the present project than the classical CCD technique. It consists in having both the photodetector function and some first stage of electronic processing functions, implanted in the same chip. As a result, the pixels could be readout individually, which is a tremendous advantage over the CCD technique for the present application. A first examination of this issue shows that the count rate capability of these devices are compatible with TOTEM requirements. Technically, the fabrication of CMOS arrays of  $10^3 \times 10^3$  pixels of 20–30  $\mu\text{m}$  is commonly achievable [10].

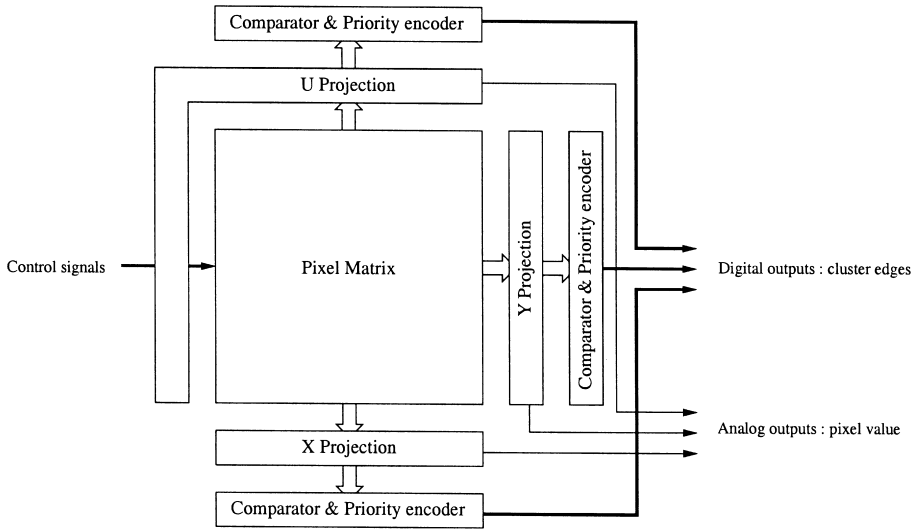


Fig. 2. Principle of the front-end electronics.

## 6.2. Front-end electronics

The pixel matrix (Fig. 2) has a common output line for all pixel within each row  $x$ , column  $y$  and diagonal  $u$ , the latter to remove  $xy$  ambiguities in multihit events. The three projections are readout in two phases, fast digital and slow analog. In the first phase the outputs of the projection banks are fed into comparators which detect signals above a given threshold. This logical representation is then encoded to provide the binary addresses of the detected clusters edges. The digital output will be used as a relatively fast first level trigger and as a first cluster selection in order to reject background hits. The second phase consists of the analog readout of the selected clusters projections that will be fed into a signal processing stage with the purpose of calculating with the maximum allowed accuracy the hit position coordinates in  $x$  and  $y$  directions. The feasibility of the project is under study at IMEC (Leuven) [10].

## 7. Angular calibration of the apparatus

A highly critical point for the reliability of the Physics measurements is the mechanical cali-

bration of the apparatus [3–5]. This arises from the ambiguity between absolute detector position with respect to the beam axis and relative mechanical position of the detectors on each side of the beam. It may generate severe angle measurement errors [3–5]. In the present scenario, this difficulty would be solved rather easily since the edges of each primary scintillator would be seen by both photodetector system, over a range which depends on the optics, and which should be optimized in the final design.

## 8. Roman pots

In order to satisfy the requirements enumerated in the introduction, the roman pots should be designed so as to avoid any matter between the phosphor radiator and the beam. In particular, one should try to avoid the metal-foil separation serving as vacuum interface as it was usually done in previous experiments of this type.

In the present case, the apparatus lends itself pretty well to such an arrangement since the lens could be used as a vacuum interface. This would imply the primary radiator and the mirror to be under the ultra-vacuum of the collider ring, which

would constrain the choice of the materials used in this part and require a rigorous procedure for any intervention on the instrumentation. Fig. 1 illustrates schematically the type of mechanical arrangement which could be used to this purpose.

## 9. Conclusion

In this first approach of a scenario based on optoelectronic detectors, we have seen that the proposed apparatus complies with all the requirements of the experiment, each element of the design having better spatial resolution performances than demanded. We believe that most of the usual techniques would be in trouble in this particular experimental situation, on one or more of the key points enumerated in the introduction. We also believe that these prospects are interesting enough to be further investigated and a R&D program based on this scheme is now underway at the ISN Grenoble.

## References

- [1] M. Bozzo et al., Total cross section, elastic scattering and diffractive dissociation at LHC, Letter of Intent, Report CERN/LHCC 97-49, 15 August 1997. A. Faus-Golfe, Study of a high  $\beta$  insertion optics for the TOTEM experiment, LHC Project Notes 145 and 152.
- [2] G. Matthiae, TOTEM measurements of low  $t$  elastic scattering, TOTEM Internal Note, 5 September 1998.
- [3] C. Augier et al., Phys. Lett. B 316 (1993) 448.
- [4] C. Augier et al., Nucl. Instr. and Meth. A 389 (1997) 409.
- [5] M. Haguenaer, private communication.
- [6] I.P. Csorba, Image Tubes, H.W. Sams and Co, Inc, Indianapolis, 1985.
- [7] G. Sorce, private communication, see <http://www.phosphor.demon.co.uk>.
- [8] J. Ballon et al., Nucl. Instr. and Meth. A 338 (1994) 310.
- [9] R.J. Hertel, Intagliated phosphor screen image tube project, Report A8127422, ITT Aerospace Optical Division, 15 May 1982.
- [10] B. Dierickx, Nucl. Instr. and Meth. A 305 (1991) 561, and private communication.